Tunable Thermal Expansion from Negative, Zero, to Positive in Cubic Prussian Blue Analogues of $GaFe(CN)_6$

Qilong Gao,[†,‡] Naike Shi, [†,‡] Andrea Sanson,[§] Yu Sun, [†,‡] Ruggero Milazzo,[§] Luca Olivi,[⊥] He Zhu,[†,‡] Saul H. Lapidus, [∥] Jun Chen,*[, †,‡] and Xianran Xing[†,‡]

[†]Beijing Advanced Innovation Center for Materials Genome Engineering, University of Science and Technology Beijing, Beijing 100083, China

[‡]Department of Physical Chemistry, University of Science and Technology Beijing, Beijing 100083, China

[§]Department of Physics and Astronomy, University of Padova, Padova I-35131, Italy

[⊥]Elettra Sincrotrone Trieste, 34149 Basovizza, Italy

[∥]Argonne National Laboratory, X-ray Science Division, Argonne, Illinois 60439, United States

Supporting Information Placeholder

ABSTRACT: The control of thermal expansion of open-framework Prussian blue analogues is vital but remains challenging. The present work proposes an effective method to control the thermal expansion, in which guest ions (Na^+) and molecules (H_2O) can adjust the coefficient of thermal expansion from strong negative, to near zero, to positive in $GaFe(CN)_6$ Prussian blue analogues. Direct experimental evidence by high-resolution synchrotron X-ray diffraction and X-ray absorption fine structure shows that the guest ions or molecules have intense dampening effect on the transverse vibrations of -Fe-C≡N-Ga- linkages responsible for NTE, especially for N atoms. The role of guests in controlling thermal expansion is attributed to the strong interaction of local environment – steric dampening. The present study demonstrates that electrochemical or redox intercalation of guest ions can be a general and effective method for controlling thermal expansion for those open-framework materials with negative thermal expansion driven by low Frequency phonons.

Control of thermal expansion is an important issue for materials. The inherent physical property of thermal expansion generally correlates with phonons, electrons, orbitals, spin, and so on. It is also affected by other macroscopic factors like nano-size, defects, and stress.[1] Negative thermal expansion (NTE) is a novel phenomenon, which brings a chance to control thermal expansion of many materials.[2,3] NTE has achieved a great progress in the last two decades, and many NTE materials have been found.[4,5] For the issue of controlling thermal expansion of NTE materials, chemical substitution is a general used method.[1] In fact, thermal expansion has been effectively tuned for those electronic-state-driven NTE functional materials, like intermetallic charge-transfer in $BiNiO_3$,[6] Mott phase transition in Ca_2RuO_4,[7,8] magnetovolume effect in magnetics alloy,[9-11] spontaneous volume ferroelectrostriction in $PbTiO_3$-based ferroelectrics.[12-14] However, for many open-framework NTE materials whose NTE is driven by low-frequency phonons, the chemical substitution is not a promising method. For example, the linear coefficient of thermal expansion (CTE, a_l) of $Zr_{1-x}M_xW_2O_{8-y}$ (M = Sc, In, Y) only varies over a narrow range (-7.3 to $-8.7\times10^{-6}K^{-1}$).[15] For systems strongly related to transverse vibrations, the control of thermal expansion should be based on structural properties, i.e., by inserting guest ions or molecules into the empty spaces of the framework structure we can hinder the transverse vibrations and thus change the thermal expansion. Based on these understanding, we achieved the control of thermal expansion in the ScF_3-based simple structure materials by inserting and removing Li ions,[16] and we also switched the thermal expansion from negative to giant positive in $YFe(CN)_6$-based Prussian blue analogues through the insertion of K ions and H_2O molecules.[17]

Prussian blue analogues (PBAs) are the well-known molecular perovskites and classic coordination compounds, which have many applications in magnetism,[18] energy and environment,[19,20] medicine,[21] and so on. Interesting NTE properties have been discovered in various PBAs, such as $FeCo(CN)_6$,[22] $Ag_3Co(CN)_6$,[23] and $YFe(CN)_6$.[17] Due to the flexible linkages of -M-C≡N-M- (M is metal), NTE of PBAs originates from the transverse vibrations of the whole CN atoms of -M-C≡N-M- linkages. Some interesting studies on the switching of thermal expansion from negative to positive in PBAs are present in the literature. For example, H_2O adsorption in $ZnPt(CN)_6$ can switch the NTE to positive thermal expansion (PTE),[24] or Rb ions and H_2O molecules interca-

lation allow to achieve zero thermal expansion (ZTE) in $Rb_{0.97}Mn[Fe(CN)_6]_{0.99}\cdot 0.3H_2O$. [25] Despite this, a satisfactory control of the thermal expansion in PBAs has not yet been achieved. In the present study, we adopt the $GaFe(CN)_6$ PBAs as a representative to realize the control of thermal expansion by guest ions and molecules. We will show that the thermal expansion of $GaFe(CN)_6$-based PBAs can be continuously tuned from strong NTE, to ZTE, to PTE through the insertion of guest Na^+ ions and H_2O molecules.

Crystal structures and thermal expansions were determined by high-resolution synchrotron X-ray diffraction (SXRD), while the role of guest ions and molecules has been investigated by Extended X-ray Absorption Fine Structure (EXAFS) spectroscopy. Like many known Prussian blue analogues, the structure of $GaFe(CN)_6$ is a cubic network with a linear bridging of alternating FeC_6 and GaN_6 octahedra (see Figure S1 in the Supporting Information). Figure 1a shows a sketch of the crystal structure. It should be noted that it is equivalent to ABX_3 perovskite, where the A-site is vacant. The NTE of $GaFe(CN)_6$ PBAs is derived from transverse thermal vibrations of CN ions, which give the shrinkage of the -Ga-C≡N-Fe- linkages (Figure 1b). We infer that if guest ions or molecules intercalation led to sterically hinder or reduce the transverse vibrations (Figure 1c), thus inhibiting the NTE, it will effectively control the thermal expansion.

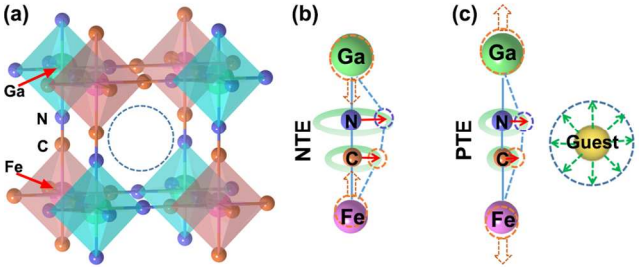

Figure 1. How the thermal expansion of $GaFe(CN)_6$ can be tuned via guest ions and molecules. (a) Sketch of the cubic structure of $GaFe(CN)_6$ consisting of alternating GaN_6 and FeC_6 octahedra. The empty space indicated by the dash circle can host guest ions or molecules. (b) The negative thermal expansion of $GaFe(CN)_6$ is derived from the transverse vibrations of CN cyanogen ions. (c) The transverse vibrations of CN cyanogen ions are hindered by guest ions or molecules, thus inhibiting the NTE and resulting in positive thermal expansion.

The insertion of Na^+ ions into the pore was performed by both Na-ions battery technology and NaI redox (details in support information). It should be noted that the guest H_2O molecules in the as-prepared sample can be removed at elevated temperature. As shown in Figure 2, $GaFe(CN)_6$ shows isotropic NTE ($\alpha_l = -3.95(5) \times 10^{-6}$ K^{-1}, 100 − 475 K). Interestingly, thermal expansion can be effectively controlled from NTE to PTE with increasing content of guest Na^+ ions and H_2O molecules. The NTE is weakened by insertion of Na^+ ions in $Na_{0.25}GaFe(CN)_6$ ($\alpha_l = -2.83(3) \times 10^{-6}$ K^{-1}) and $Na_{0.5}GaFe(CN)_6$ ($\alpha_l = -1.51(2) \times 10^{-6}$ K^{-1}). An interesting isotropic ZTE is achieved in $NaGaFe(CN)_6$ ($\alpha_l = +0.30(2) \times 10^{-6}$ K^{-1}). With further introduction of H_2O molecules, a PTE is achieved in $NaGaFe(CN)_6\cdot 2H_2O$ ($\alpha_l = +3.98(4) \times 10^{-6}$ K^{-1}). So, we can effectively tune the thermal expansion of $GaFe(CN)_6$ PBAs through controlling the concentration of guest ions or molecules.

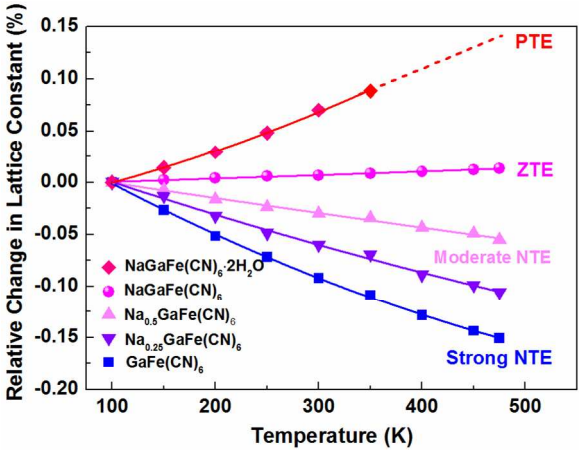

Figure 2. Temperature dependence of the relative change in lattice constant of $GaFe(CN)_6$-based compounds.

It is interesting to highlight that a wide controllable CTE range has been achieved in the present PBAs, which was rarely observed in framework materials. For example, in the ScF_3-based fluorides,[26] a linear CTE can be achieved from -3.3 to 3.3 × 10^{-6} K^{-1} through the Fe and Ga chemical substitutions. In $M^{II}Pt(CN)_6$ (Mn, Fe, Co, Ni, Cu, Zn, Cd),[27] the adjustable CTE range is from -10.02 to -1.02× 10^{-6} K^{-1}. Moreover, an interesting ZTE property is found in $NaGaFe(CN)_6$ over a wide temperature range when compared with others ZTE materials, such as $Zn_4B_6O_{13}$ (13 − 110 K),[28] $FeCo(CN)_6$ (4.2 − 300 K),[22] $Mn_{3.243}Ni_{0.747}N$ (140 −230 K).[29]

Now, we aim to gain new insights into the role of guest ions and molecules on the control of thermal expansion. For this reason, we investigate the phenomenon through the comparison between high-resolution SXRD and EXAFS spectroscopy. Firstly, let us recall that the bond length obtained by high-resolution SXRD is the so-called "apparent" bond length, while the one between neighboring atoms measured by EXAFS is the "ture" bond length. As shown in Figure 3, one can find that for $GaFe(CN)_6$ the "apparent" Ga-N and Fe-C bond lengths display NTE, while the "true" ones shows an opposite PTE as function of temperature. The difference is strictly related to the transverse thermal vibrations After the Na insertion into the pores of $GaFe(CN)_6$, the thermal expansion of Ga-N bond is dramatically affected (Figure 3a), while much less evident is the effect on the Fe-C bonds (Figure 3b). This suggests that the guest Na^+ ions has a strong effect on the lattice dynamics of Ga-N bonds, much less on that of Fe-C bonds.

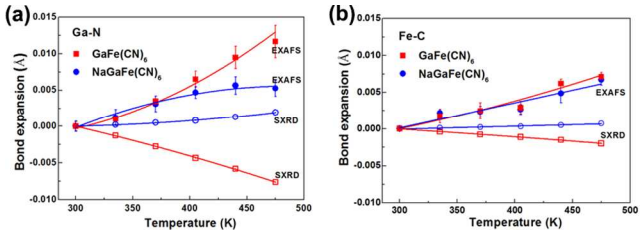

Figure 3. Temperature dependence of the relative change of chemical bonds. (a) Ga-N and (b) Fe-C bond expansion in $GaFe(CN)_6$ (red colors) and $NaGaFe(CN)_6$ (blue colors). The thermal expansion of the "true" (solid symbols) and "apparent" (open symbols) bonds is determined by EXAFS and SXRD, respectively. The solid lines are a guide to the eyes.

In order to describe the vibrational dynamics of CN cyanide, the perpendicular and parallel mean square relative displacements (MSRD) of the Ga-N and Fe-C bonds have been extracted according to well-established procedures.[30] $GaFe(CN)_6$ has a strong NTE which comes from the strong transverse thermal vibration of CN cyanide. Indeed, as shown in Figure 4a-b, the perpendicular MSRDs are much larger than the parallel MSRDs ones for both Ga-N and Fe-C bonds of $GaFe(CN)_6$. In specific, the perpendicular MSRD of Ga-N is about twice that of Fe-C at room temperature. This is a direct experiment evidence that the driving force for the NTE of $GaFe(CN)_6$ is the transverse vibrations of N and C atoms with the predominant contribution from N atoms. However, with the presence of Na in $NaGaFe(CN)_6$, the values of perpendicular Ga-N and Fe-C sharply reduce, while those of parallel ones nearly does not change. This reveals that the insertion of Na^+ ions inhibits or weakens the transverse vibrations of cyanogen (Figure 4a), with a remarkable effect on the transverse vibrations of N atoms, smaller on C atoms.

For a given atomic pair, the anisotropy of the relative thermal vibrations can be evaluated by the ratio $\gamma = MSRD_{\perp} / MSRD_{||}$. In the NTE $GaFe(CN)_6$, the ratio γ of Ga-N bonds approximate ~50 at high temperature (Figure 4c), a value much larger than other NTE materials like $CuScO_2$,[31] ZrW_2O_8 [32] or ScF_3.[33] Differently, in the ZTE $NaGaFe(CN)_6$, the ratio γ of Ga-N bonds assumes much lower values. A similar behaviour, although less pronounced, is also observed for the ratio γ of Fe-C bonds (Figure 4d). The present results reflect that Na insertion has a significant influence on the transverse vibrations of N and C atoms. The thermal ellipsoids of relative thermal vibrations of N and C atoms, reconstructed from the data reported in Figure 4a-b, are shown in Figure 4e. These ellipsoids give an immediate visualization of the large transverse vibrations of C and N atoms, perpendicular to the -Ga-N≡C-Fe- linkages. The Na^+ ions insertion weakens the transverse thermal vibrations of CN atoms, in particular for N atoms.

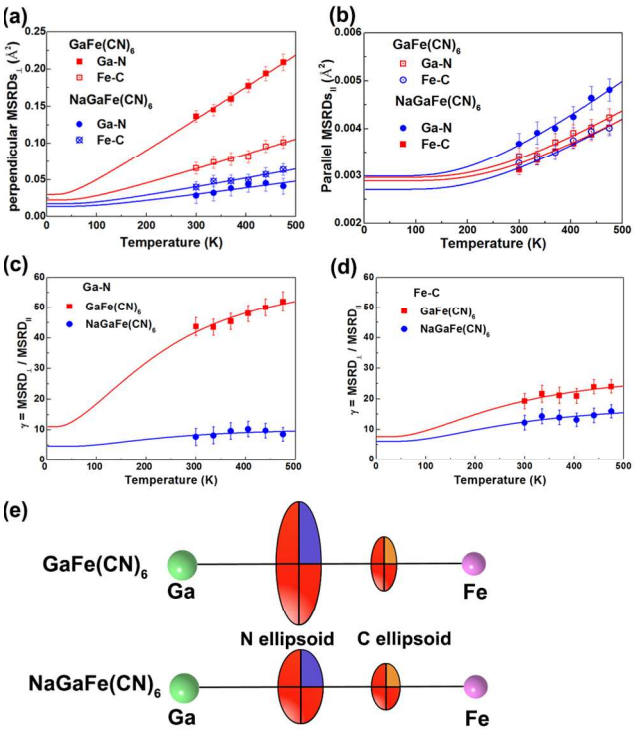

Figure 4. Local vibrational dynamics in $GaFe(CN)_6$ and $NaGaFe(CN)_6$. (a) Perpendicular $MSRD_{\perp}$, and (b) Parallel $MSRD_{//}$ of Ga − N (solid symbols) and Fe – C (open symbols) bonds. Anisotropy $\gamma = MSRD_{\perp} / MSRD_{//}$ of relative thermal vibrations of (c) Ga – N, and (d) Fe – C bonds The lines are the best fits by utilizing the Einstein model. (e) Schematic representation of the thermal ellipsoids of the relative Ga-N and Fe-C thermal vibrations in $GaFe(CN)_6$ and in $NaGaFe(CN)_6$.

A similar dampening behavior of NTE was observed in other open-framework NTE materials, such as H_2O in ZrW_2O_8,[34] CCl_4 in $Cd(CN)_2$,[35] He_2 in $CaZrF_6$,[36] and CO_2/H_2 in MOF.[37] The role of guests on NTE has been ascribed to the steric dampening effect on the transverse thermal vibration. In this work, $GaFe(CN)_6$ is used as an example to study the direct experimental evidence to such steric dampening effect. Na^+ ions weaken the transverse vibration of cyanogen, which can therefore control the thermal expansion. Furthermore, the contribution of NTE from N and C atoms has been well distinguished.

In summary, this work shows that guest Na ions or H_2O molecules can successfully control the thermal expansion of $GaFe(CN)_6$. The presence of guests in the interstitial void can significantly hinder or damp the transverse vibrations of Ga-N and Fe-C bonds, in particular for N atoms, whose contribution to NTE is dominant. This method of tuning the coefficient of thermal expansion in $GaFe(CN)_6$ PBAs could be used in other NTE materials with open-framework, such as oxides, cyanides, metal-organic frameworks, and zeolites.

ASSOCIATED CONTENT

Supporting Information. The Supporting Information is available free of charge on the ACS Publications website. Materials synthesis, Experimental details, Data analysis procedures and Supporting Figure.

AUTHOR INFORMATION

Corresponding Author

*junchen@ustb.edu.cn

Notes

The authors declare no competing financial interest.

ACKNOWLEDGMENT

This work was supported by the National Natural Science Foundation of China (Grant Nos. 21731001, 21590793), the Fundamental Research Funds for the Central Universities, China (FRF-TP-17-001B), and the Changjiang Young Scholars Award. Use of the Advanced Photon Source, an Office of Science User Facility operated for the U.S. Department of Energy (DOE) Office of Science by Argonne National Laboratory, was supported by the U.S. DOE under Contract No. DE-AC02-06CH11357. ELETTRA Synchrotron is acknowledged for provision of synchrotron radiation (Experiment 20170167), as well as all the staff of XAFS Beamline for technical assistance.

REFERENCES

(1) Chen, J.; Hu, L.; Deng, J. X.; Xing, X. R. Negative Thermal Expansion in Functional Materials: Controllable Thermal Expansion by Chemical Modifications. *Chem. Soc. Rev.* **2015**, *44*, 3522–3567.

(2) Mary, T. A.; Evans, J. S. O.; Vogt, T.; Sleight, A. W. Negative Thermal Expansion from 0.3 to 1050 Kelvin in ZrW_2O_8. *Science* **1996**, *272*, 90–92.

(3) Attfield, J. P. Condensed-matter Physics: A Fresh Twist on Shrinking Materials. *Nature 2011*, *480*, 465–466.

(4) Dove, M. T.; Fang, H. Negative Thermal Expansion and Associated Anomalous Physical Properties: Review of the Lattice Dynamics Theoretical Foundation. *Rep. Prog. Phys.* **2016***, 79*, 066503.

(5) Lind, C. Two Decades of Negative Thermal Expansion Research: Where Do We Stand? *Materials*. **2012**, *5*, 1125–1154.

(6) Azuma, M.; Chen, W. T.; Seki, H.; Czapski, M.; Oka, K.; Mizumaki, M.; Watanuki, T.; Ishimatsu, N.; Kawamura, N.; Ishiwata, S.; Tucker, M. G.; Shimakawa, Y.; Attfield. J. P. Colossal Negative Thermal Expansion in $BiNiO_3$ Induced by Intermetallic Charge Transfer. *Nature Commun*. **2011**, *2*, 347.

(7) Takenaka, K.; Okamoto, Y.; Shinoda, T.; Katayama, N.; Sakai, Y. Colossal Negative Thermal Expansion in Reduced Layered Ruthenate. *Nat. Commun.* **2017**, *8*, 14102.

(8) Braden, M.; Andre, G.; Nakatsuji, S.; Maeno, Y. Crystal and Magnetic Structure of Ca_2RuO_4: Magnetoelastic Coupling and the Metal-insulator Transition. *Phys. Rev. B*. **1998**, *58*, 847–861.

(9) Wang, C.; Chu, L.; Yao, Q.; Sun, Y.; Wu, M.; Ding, L.; et al. Tuning the Range, Magnitude, and Sign of the Thermal Expansion in Intermetallic $Mn_3(Zn, M)_xN$ (M= Ag, Ge). *Phys. Rev. B*, **2012**, *85*, 220103.

(10) Takenaka, K.; Takagi, H. Giant Negative Thermal Expansion in Ge-doped Anti-perovskite Manganese Nitrides. *Appl. Phys. Lett.* **2005**, *87*, 261902.

(11) Song, Y.; Chen, J.; Liu, X.; Wang, C.; Zhang, J.; Liu, H.; Zhu, H.; Hu, Lei; Lin, Kun.; Zhang, S.; Xing, X. R. Zero Thermal Expansion in Magnetic and Metallic $Tb(Co, Fe)_2$ Intermetallic Compounds. *J. Am. Chem. Soc.* **2018**, *140*, 602–605.

(12) Chen, J.; Wang, F.; Huang, Q.; Hu, L.; Song, X.; Deng, J. X.; Yu, R. B.; Xing, X. R. Effectively Control Negative Thermal Expansion of Single-phase Ferroelectrics of $PbTiO_3$-$(Bi, La)FeO_3$ Over a Giant Range. *Sci. Rep*. **2013**, *3*, 2458.

(13) Chen, J.; Xing, X. R.; Sun, C.; Hu, P. H.; Yu, R. B.; Wang, X. W.; Li, L. H. Zero Thermal Expansion in $PbTiO_3$-based Perovskites. *J. Am. Chem. Soc*. **2008**, *130*, 1144–1145.

(14) Pan, Z.; Chen, J.; Jiang, X.; Hu, L.; Yu, R. Z.; Yamamoto, H.; Ogata, T.; Hattori, Y.; Guo, F. M.; Fan, X.; Li, Y.; Li, G.; Gu, H; Ren, Y.; Lin, Z.; Azuma, M.; Xing, X. R. Colossal Volume Contraction in Strong Polar Perovskites of $Pb(Ti, V)O_3$. *J. Am. Chem. Soc*. **2017**, *139*, 14865–14868.

(15) Nakajima, N.; Yamamura, Y.; Tsuji, T. Synthesis and Physical Properties of Negative Thermal Expansion Materials $Zr_{1-x}M_xW_2O_{8-y}$ (M = Sc, In, Y) Substituted for Zr (IV) Sites by M (III) Ions. *Solid State Commun.* **2003**, *128*, 193–196.

(16) Chen, J.; Gao, Q. L.; Sanson, A.; Jiang, X. X.; Huang, Q. Z.; Carnera, A.; Rodriguez, C. G.; Olivi, L.; Wang, L.; Hu, L.; Lin, K.; Ren, Y.; Lin, Z. S.; Wang, C.; Gu, L.; Deng, J. X.; Attfield, J. P.; Xing, X. R. Tunable Thermal Expansion in Framework Materials Through Redox Intercalation. *Nat. Commun*. **2017**, *8*, 14441.

(17) Gao, Q. L.; Chen, J.; Sun, Q.; Chang, D. H.; Huang, Q. Z.; Wu, H.; Sanson, A.; Milazzo, R.; Zhu, H.; Li, Q.; Liu, Z. N.; Deng, J. X.; Xing, X. R. Switching between Giant Positive and Negative Thermal Expansions of a $YFe(CN)_6$-based Prussian Blue analogue Induced by Guest Species. *Angew. Chem. Int. Ed.* **2017**, *56*, 9023-9028.

(18) Ohkoshi, S.; Tokoro, H.; Matsuda, T.; Takahashi, H.; Irie, H.; Hashimoto, K. Coexistence of Ferroelectricity and Ferromagnetism in a Rubidium Manganese Hexacyanoferrate. *Angew. Chem.* **2007**, *119*, 3302–3005.

(19) Kaye, S. S.; Long, J. R. Hydrogen Storage in the Dehydrated Prussian Blue Analogues $M_3[Co(CN)_6]_2$ (M = Mn, Fe, Co, Ni, Cu, Zn). *J. Am. Chem. Soc.* **2005**, *127*, 6506-6507.

(20) Gao, Q. L.; Chen, J.; Li, Q.; Zhang, J.; Zhai, Z.; Zhang, S. T.; Yu, R. B.; Xing, X. R. Structure and Excellent Visible Light Catalysis of Prussian Blue Analogues $BiFe(CN)_6{\cdot}4H_2O$. *Inorg. Chem. Front.* **2018**, *5*, 438–445.

(21) Patra, C. R. Prussian Blue Nanoparticles and Their Analogues for Application to Cancer Theranostics. *Nanomedicine.* **2016**, *11*, 569–572.

(22) Margadonna, S.; Prassides, K.; Fitch, A. N. Zero Thermal Expansion in a Prussian Blue Analogue. *J. Am. Chem. Soc.* **2004**, *126*, 15390–15391.

(23) Goodwin, A. L.; Calleja, M.; Conterio, M. J.; Dove, M. T.; Evans, J. S.; Keen, D. A.; et al. Colossal Positive and Negative Thermal Expansion in the Framework Material $Ag_3[Co(CN)_6]$. *Science*. **2008**, *319*, 794-797.

(24) Goodwin, A. L.; Chapman, K. W.; Kepert, C. J. Guest-dependent Negative Thermal Expansion in Nanoporous Prussian Blue Analogues $M^{II}Pt^{IV}(CN)_6{\cdot}x\{H_2O\}(0 \le x \le 2$; M = Zn, Cd). *J. Am. Chem. Soc.* **2005**, *127*, 17980–17981.

(25) Tokoro, H.; Nakagawa, K.; Imoto, K.; Hakoe, F.; Ohkoshi, S. I. Zero Thermal Expansion Fluid and Oriented Film Based on a Bistable Metal-cyanide Polymer. *Chem. Mater*. **2012**, *24*, 1324−1330.

(26) Hu, L.; Chen, J.; Fan, L.; Ren, Y.; Rong, Y.; Pan, Z., Deng, J. X.; Yu, R.; Xing, X. R.. Zero Thermal Expansion and Ferromagnetism in Cubic $Sc_{1-x}M_xF_3$ (M = Ga, Fe) Over a Wide Temperature Range. *J. Am. Chem. Soc*. **2014**, *136*, 13566-13569.

(27) Chapman, K. W.; Chupas, P. J.; Kepert, C. J. Compositional Dependence of Negative Thermal Expansion in the Prussian Blue Analogues $M^{II}Pt^{IV}(CN)_6$ (M = Mn, Fe, Co, Ni, Cu, Zn, Cd). *J. Am. Chem. Soc*. **2006**, *128*, 7009-7014.

(28) Jiang, X. X.; Molokeev, M. S.; Gong, P.; Yang, Y.; Wang, W.; Wang, S. H.; et al. Near-zero Thermal Expansion and High Ultraviolet Transparency in a Borate Crystal of $Zn_4B_6O_{13}$. *Adv. Mater.* **2016**, *28*, 7936–7940.

(29) Deng, S.; Sun, Y.; Wu, H.; Huang, Q.; Yan, J.; Shi, K.; et al. Invar-like Behavior of Antiperovskite $Mn_{3+x}Ni_{1-x}N$ Compounds. *Chem. Mater.* **2015**, *27*, 2495–2501.

(30) Fornasini, P.; Grisenti, R. On EXAFS Debye-Waller Factor and Recent Advances. *J. Synchrotron Rad.* **2015**, *22*, 1242−1257.

(31) Ahmed, S. I.; Dalba, G.; Fornasini, P.; Vaccari, M.; Rocca, F.; Sanson, A.; et al. Negative Thermal Expansion in Crystals with the Delafossite Structure: An Extended X-ray Absorption Fine Structure Study of $CuScO_2$ and $CuLaO_2$. *Phys. Rev. B*. **2009**, *79*, 104302.

(32) Sanson, A. Toward an Understanding of the Local Origin of Negative Thermal Expansion in ZrW_2O_8: Limits and Inconsistencies of the Tent and Rigid Unit Mode Models. *Chem. Mater*. **2014**, *26*, 3716–3720.

(33) Hu, L.; Chen, J.; Sanson, A.; Wu, H.; Guglieri Rodriguez, C.; Olivi, L.; Ren, Y.; Fan, L. L.; Deng, J. X.; Xing, X. R. New Insights into the Negative Thermal Expansion: Direct Experimental Evidence for the "Guitar-String" Effect in Cubic ScF_3. *J. Am. Chem. Soc*. **2016**, *138*, 8320–8323.

(34) Duan, N.; Kameswari, U.; Sleight, A. W. Further Contraction of ZrW_2O_8. *J. Am. Chem. Soc*. **1999**, *121*, 10432–10433.

(35) Phillips, A. E.; Goodwin, A. L.; Halder, G. J.; Southon, P. D.; Kepert, C. J. Nanoporosity and Exceptional Negative Thermal Expansion in Single-network Cadmium Cyanide. *Angew. Chem. Int. Ed.* **2008**, *120*, 1418−1421.

(36) Hester, B. R.; Dos Santos, A. M.; Molaison, J. J.; Hancock, J. C.; Wilkinson, A. P. Synthesis of Defect Perovskites $(He_{2-x}\square_x)(CaZr)F_6$ by Inserting Helium into the Negative Thermal Expansion Material $CaZrF_6$. *J. Am. Chem. Soc*. **2017**, *139*, 13284–13287.

(37) Queen, W. L.; Brown, C. M.; Britt, D. K.; Zajdel, P.; Hudson, M. R.; Yaghi, O. M. Site-specific CO_2 Adsorption and Zero Thermal Expansion in an Anisotropic Pore Network. *J. Phys. Chem. C.* **2011**, *115*, 24915–24919.

TOC

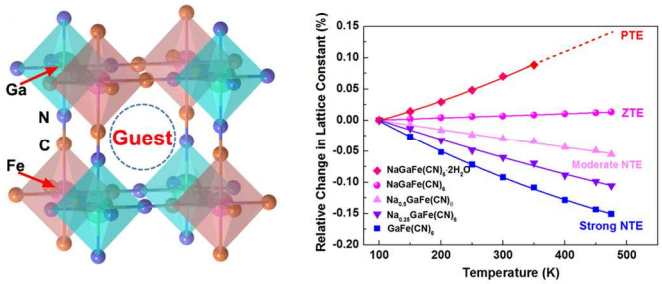
Ga
N
C
Fe
Guest
PTE
ZTE
Moderate NTE
Strong NTE
Relative Change in Lattice Constant (%)
Temperature (K)
0.15
0.10
0.05
0.00
-0.05
-0.10
-0.15
-0.20
100
200
300
400
500